

# AUTOMATIC ASSESSMENT OF MAMMOGRAPHIC POSITIONING ON THE MEDIOLATERAL OBLIQUE VIEW

*Sze Man Kwok, Ramachandran Chandrasekhar and Yianni Attikiouzel*

Centre for Intelligent Information Processing Systems  
School of Electrical, Electronic and Computer Engineering  
The University of Western Australia, Crawley, WA 6009, Australia

kwok-sm|chandra|yianni@ee.uwa.edu.au

## ABSTRACT

Mammograms are X-ray images of the compressed breast and are widely used for early detection of breast cancer. A mammogram must be of sufficient quality for the radiologist to detect lesions or other abnormalities with high sensitivity and specificity. In this paper, some algorithms are presented for the automatic assessment of the quality of positioning on mediolateral oblique (MLO) view mammograms. Anatomic features, including the breast border, nipple location and pectoral margin, were first extracted from each image. Then several quality criteria, including breast tissue exclusion, nipple in profile, inclusion of inframammary fold, and positioning of the pectoral muscle, were used to assess the adequacy of breast positioning. The assessment method was tested on 322 digitized mammograms in the MIAS database.

## 1. INTRODUCTION

Achieving high image quality is essential to the radiologist who wants to interpret the mammogram with high sensitivity and specificity [1]. We believe that image quality assessment is an important component in the computerized analysis of mammograms. Low-quality mammograms may adversely affect the performance of automatic segmentation and the accuracy of cancer detection. Inadequate images may not contain sufficient diagnostic information and should be identified as early as possible so that they are not subjected to further analysis.

Although the assessment of mammographic image quality usually requires some subjective considerations, there is a consensus in the literature [1, 2, 3] on the *quality attributes* that an ideal mammogram should incorporate. A high quality mammogram should exhibit correct positioning, optimal compression, good contrast, adequate exposure, low noise, high sharpness, and absence of artefacts [3]. Chief among these attributes is *positioning*, which crucially determines the amount of tissue inclusion [1] and correlates with the overall quality of the mammogram [3].

Several algorithms for the assessment of the quality of positioning are presented in this paper. An earlier version of this work was presented in [4]. However, our literature searches have not revealed other published accounts of systems for automatically assessing the adequacy of mammographic positioning.

## 2. OPTIMAL POSITIONING IN THE MLO VIEW

The mediolateral oblique (MLO) view is considered by radiologists to be the most important view, in which all of the breast tissue

is most likely to be included on the film [1]. To ensure that the entire glandular body is imaged with the best possible compression, *correct positioning* of the breast is a pre-requisite [2]. Exclusion of glandular tissues from the field of view could increase the risk of missing lesions, or abnormalities. In fact, one recent study on clinical image quality and the risk of interval cancer has shown that “invasive breast cancer detection by mammography may be improved through attention to correct positioning” [3].

Optimal positioning can be achieved in the MLO view when a number of *quality criteria* are fulfilled. These criteria are described in most detail in [1] and also outlined elsewhere [2, 3]. They are illustrated in Fig. 1(a). In the figure, (1) the pectoral muscle is visible at least to the level of the nipple (dotted line); (2) the angle between the pectoral margin and the posterior image edge is at least  $20^\circ$ ; (3) the anterior pectoral margin is convex when the pectoral muscle was fully mobilized and maintained medially during compression and image acquisition; (4) the inframammary fold is included on the image to ensure that the lower posterior tissue has not been excluded; (5) the posterior glandular tissue is separated from the image edge by retroglandular fat; (6) upper glandular tissue superimposed over the upper pectoral muscle is not excluded in the view; and (7) the nipple is preferably seen in profile in at least one of the standard views.

Quality criteria (1)–(3) are for assessing the positioning of the pectoral muscle; while (4)–(6) are for preventing the exclusion of glandular tissue at the posterior image edge. In addition, glandular tissue should not be excluded at the anterior and inferior image edges. These exclusions are more obvious than the posterior one since part of the skin-air interface is missing from the image. All of the quality criteria mentioned above were evaluated by computer in this assessment, except for (5) and (6) for which the accurate, automatic outlining of glandular tissue was not currently available.

## 3. MEASURING THE QUALITY OF POSITIONING

### 3.1. Image Orientation and Notation

The image orientation and notation used in the positioning assessment algorithms are illustrated in Fig. 1(b). For consistency, the image orientation and co-ordinate system are the same as those used in pectoral muscle segmentation. All images are oriented so that they are upright and the nipple faces the right. The origin of the co-ordinate system is at the top left corner of the image, where  $x$  is defined to be the horizontal axis and  $y$  to be the vertical one. The breast border that consists of  $n$  pixels is represented by a dis-

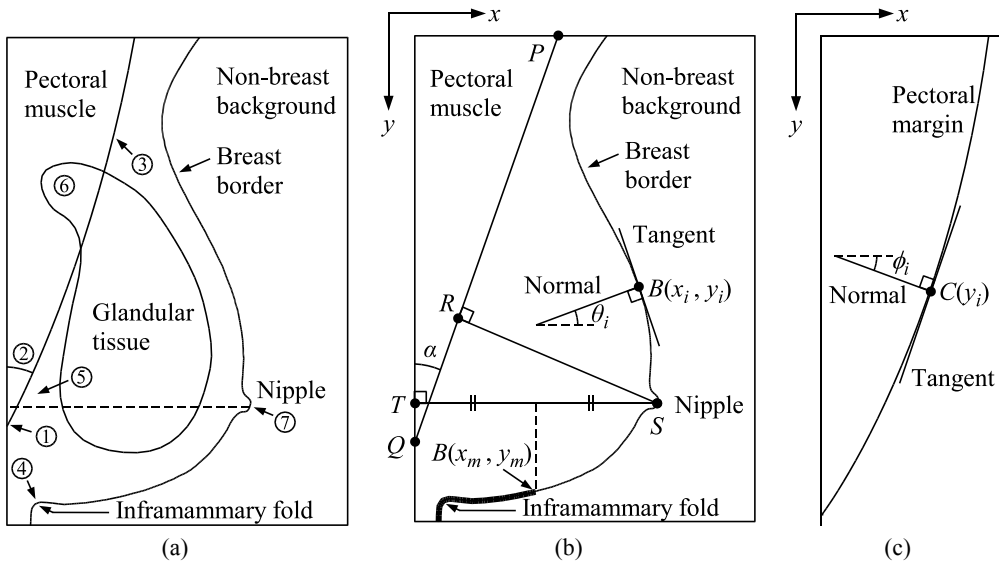


**Fig. 1.** (a) Quality criteria for optimal positioning in the MLO view; the numbers correspond to the criteria enumerated in section 2. (b) Image orientation and notation used in the algorithms that we have devised. (c) Notation used for measuring the curvature of the pectoral margin.

crete function  $B(x_i, y_i)$  for  $i = 0, \dots, n - 1$ ; running from top to bottom. All the normals to the border are directed inwards to the breast. The angle of each normal,  $\theta_i$ , in the range  $[180^\circ, -180^\circ]$ , is positive when measured anti-clockwise from positive  $x$ -axis and negative when measured clockwise.

### 3.2. Exclusion of Breast Tissue

Although the exclusion of breast tissue at the posterior edge of the image cannot be detected unless an accurate outline of dense glandular tissue is available, the breast tissue exclusion at the anterior and inferior edges of the image can be identified by examining the breast border. The breast border was extracted from the image by background modelling and subtraction [5]. If part of the breast is excluded at the image edge, a segment of the breast border would be in the form of a horizontal or vertical straight line rather than a curve, and would be found very close to the image edge (see Fig. 2(a)).

In our algorithm, breast tissue exclusion is detected by first estimating the tangent at each point on the breast border. The tangent is estimated by fitting a straight line (using least squared error) to  $B(x, y)$  within a neighbourhood of 10 mm centred on  $(x_i, y_i)$ . The normal to  $B(x, y)$  is then directed perpendicular to the tangent, pointing inwards to the breast region. The angle measured from the positive  $x$ -axis to the normal is denoted by  $\theta_i$  in the range  $[180^\circ, -180^\circ]$ . Finally, exclusion of breast tissue is detected when there exists a segment on  $B(x, y)$  so that (i) all the normals in that segment are either horizontal or vertical, i.e.,  $\theta_i$  is either  $0^\circ$  or  $-90^\circ$ ; and (ii) the segment is at least 10 mm long; and (iii) the segment is within a 5 mm margin of the anterior and inferior image edges.

### 3.3. Nipple in Profile

The algorithm used to locate the nipple and to determine whether it is in profile is described in [6]. A brief explanation of the basis of that method is given here. If the nipple is in profile, it is depicted as a small semi-circle on the breast border; otherwise it is not seen on the breast border (see Fig. 2(b)). With this distinctive feature, the nipple is inferred to be in profile by the algorithm when the change of normal direction near the nipple is higher than usual, i.e., when the maximum change is over an absolute threshold, defined in [6].

### 3.4. Locating the Inframammary Fold

Based on general observation, when the inframammary fold exists, a distinctive concave curve can be found on the border near the lower posterior region; otherwise the breast border is only a slightly convex curve. Therefore the inframammary fold can be located by examining the curvature of the breast border (see Fig. 2(b)).

Because the inframammary fold is at the lower posterior breast region, only a portion of the breast border is included for examination (shown as thickened line in Fig. 1(b)). This portion is defined on  $B(x_i, y_i)$  for  $i = m, \dots, n - 1$  where  $x_m$  is half of the maximum horizontal distance between the breast border and posterior image edge. The maximum horizontal distance does not necessarily coincide with the nipple location. After defining the examination area, the change of normal direction,  $\theta'_i$ , is computed using the following equation:

$$\theta'_i = \begin{cases} \theta_i - \theta_{i-1} & \text{if } i > 0 \\ \theta_{i+1} - \theta_i & \text{if } i = 0 \end{cases} \quad (1)$$

All concave segments on  $B(x, y)$  which have  $\theta'$  greater than zero are then labelled. The inframammary fold is detected when there exists one or more labelled segments which are at least 10 mm

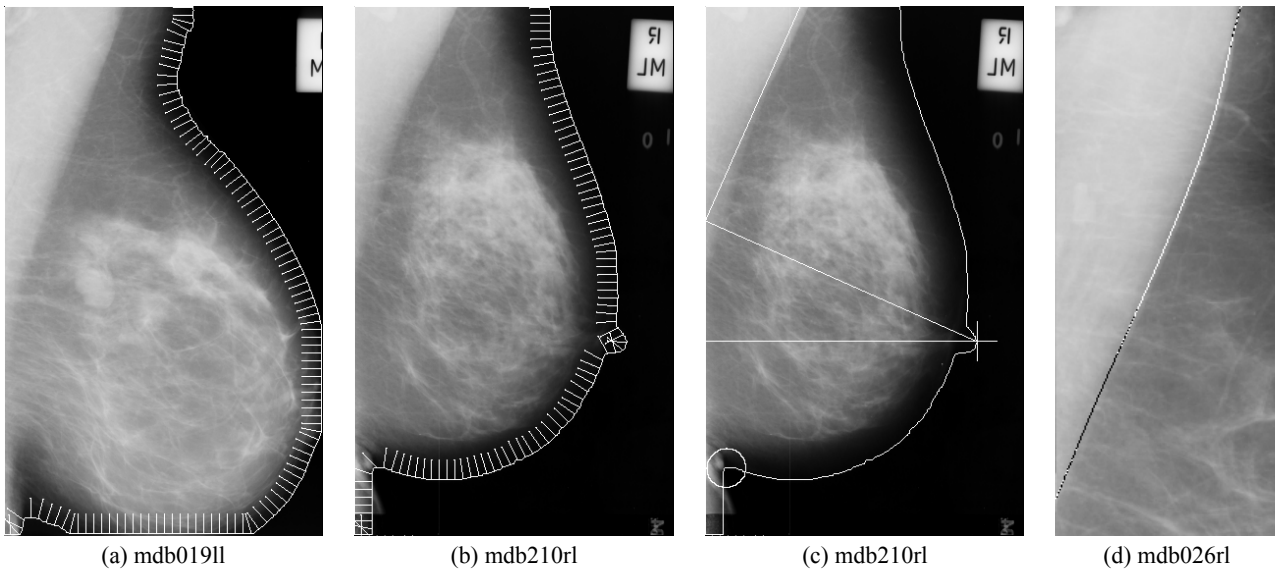


**Fig. 2.** (a) The normals to the breast border are either horizontal or vertical at the sections where the breast is excluded from the image (only every 8th normal is shown). (b) Distinctive changes on the border curvature indicate whether the nipple is in profile and whether the inframammary fold is included. (c) One of the results generated by computer. The nipple location is marked by a cross; the inframammary fold is circled; the pectoral muscle is not seen to the level of the nipple; the angle of pectoral margin is  $23.9^\circ$ ; the length of posterior nipple line is 121mm. (d) Convexity (white) and concavity (black) of the pectoral margin; 66% of the curve was determined convex.

long. Finally, the location of the inframammary fold is determined at the midpoint of the labelled segment that is maximum in length.

### 3.5. Positioning of the Pectoral Muscle

To determine whether the pectoral muscle is visible to the level of the nipple or below, two straight lines are drawn on the image. The first straight line approximating the pectoral margin is given by an automatic segmentation algorithm described in [7]. It is denoted as  $\overline{PQ}$  in Fig. 1(b). The second straight line representing the level of the nipple is drawn horizontally from the nipple to the posterior image edge, denoted as  $\overline{ST}$ . If the pectoral muscle is adequately imaged, it will be visible to the level of the nipple or below, and point  $Q$  should be at the same level or below point  $T$ .

The angle between the pectoral margin and the posterior image edge is denoted by  $\alpha$  in Fig. 1(b). This angle is measured anti-clockwise from  $\overline{PQ}$  to the vertical edge. For adequate positioning, the angle should be  $20^\circ$  or greater [2].

The posterior nipple line for the MLO view is defined in [1] as “the distance from the nipple-skin junction to the pectoral muscle or to the back of the image, whichever comes first.” This line should be drawn along the nipple axis, but can be approximated by a straight line,  $\overline{RS}$ , drawn perpendicularly from the nipple to  $\overline{PQ}$ . If  $\overline{PQ}$  and  $\overline{RS}$  intersect outside of the image domain, the posterior nipple line is only measured from the nipple to the posterior image edge. Measuring the posterior nipple line is *not* required in the positioning assessment of the MLO view, but it is a useful comparative feature in the positioning assessment of another mammographic view, the *craniocaudal view* [1].

### 3.6. Curvature of the Pectoral Margin

The pectoral margin can be accurately delineated by refining the pectoral straight line into a curve using an iterative method described in [7]. The curvature of the the pectoral margin is measured by examining the normal directions of all the pixels on the pectoral curve (see Fig. 1(c)). For every point on the pectoral curve,  $C(y)$ , the tangent at  $y_i$  is estimated by fitting a straight line (using least squared error) to  $C(y)$  within a neighbourhood of 40 mm centred on  $y_i$ . The normal to each point on  $C(y)$ , directed inwards to the pectoral region, is then computed by finding the line perpendicular to the corresponding tangent. The angle of each normal is denoted by  $\phi_i$  in the range  $[180^\circ, -180^\circ]$ . Like  $\theta_i$ ,  $\phi_i$  is positive when measured anti-clockwise from the positive  $x$ -axis and negative when measured clockwise. The change of the normal direction at  $y_i$  is represented by  $\phi'_i$  which is given by:

$$\phi'_i = \begin{cases} \phi_i - \phi_{i-1} & \text{if } i > 0 \\ \phi_{i+1} - \phi_i & \text{if } i = 0 \end{cases} \quad (2)$$

If  $\phi'_i$  is negative or zero, the pectoral curve is determined convex at  $y_i$ ; otherwise it is concave. The segmented pectoral margin usually exhibits a mixture of convexity and concavity. Therefore its overall curvature can be represented by the percentage of convex sections in the curve  $C(y)$ . An example is shown in Fig. 2(d).

## 4. RESULTS

The positioning assessment algorithms were tested on all 322 images in the MIAS database [8]. The original  $50 \mu\text{m}/\text{pixel}$  images were reduced in resolution to  $400 \mu\text{m}/\text{pixel}$  by averaging  $8 \times 8$  pixels to one. The original 8-bit grey levels were retained.

**Table 1.** Number of MIAS Images Fulfilling the Quality Criteria

Quality Criteria	No./Total	Percent
(a) No breast tissue excluded	256/322	79.5%
(b) Nipple in profile	93/322	28.9%
(c) Inframammary fold included	121/322	37.6%
(d) Pectoral margin to level of nipple	6/316	1.9%
(e) Angle of pectoral margin $\geq 20^\circ$	216/316	68.4%
(f) Convexity of pectoral margin $\geq 50\%$	207/316	65.5%
All criteria satisfied	2/322	0.6%
All criteria satisfied except for (d)	15/322	4.7%

The results of the assessment are summarized in Table 1. They are labelled from (a) to (f). Some of the criteria, (a), (e) and (f), were satisfied by the majority of the images; while the others, (b)–(d), were fulfilled by relatively few images. Only two images in the database were found satisfying all six criteria, due to the fact that the pectoral muscle was rarely seen to the level of the nipple (d). When criterion (d) was excluded from the assessment, the quality criteria could be fulfilled by 15 images, but that is still very few out of the whole set of 322 images. The 50% cut-off point used in (f) is not a standard in the clinical references but was rather subjectively set for the purposes of this assessment.

## 5. DISCUSSION

The algorithms were found to be reliable for detecting the exclusion of breast tissue at the anterior and inferior image edges, the profile of nipple and the inframammary fold, provided the breast border was accurately extracted from the image. The curvature of the pectoral muscle could also be measured precisely with the proposed method, provided the pectoral curve was accurately extracted. Therefore the segmentation of the anatomic features of the breast is an important pre-processing step for the assessment of positioning quality, since the latter is *highly dependent* on the accuracy of the segmentation of the breast border and the pectoral curve [9].

The quality criterion for the pectoral muscle to be seen to the level of the nipple was fulfilled by relatively few images in the MIAS database. Given the importance of this criterion, it must be inferred that very few images in the MIAS database are diagnostically adequate. Since the quality measures used in this paper are quantitative, perhaps they should be weighted and summed in the future with an analog scale of adequacy as suggested by Taplin et al. [3], to provide a figure-of-merit for the overall positioning quality of the mammogram.

We also envisage the possibility of real-time implementation of the system in a mammogram screening clinic where the adequacy assessment is performed before the subject leaves the clinic.

## 6. CONCLUSIONS

The adequacy of breast positioning was automatically evaluated on 322 digitized mammograms using several quality criteria. The purpose of this assessment was not only to investigate the quality of the MIAS images, but also to demonstrate a proof-of-concept that

mammographic image quality can be assessed by computer. The algorithms developed in this paper were found to be reliable and precise. In future, they should be extended to cover the craniocaudal view and other quality factors, such as exposure and contrast, and ultimately weighted and summed to provide a global figure-of-merit for mammogram adequacy.

## 7. REFERENCES

- [1] G W Eklund, Gilda Cardenosa, and Ward Parsons, "Assessing Adequacy of Mammographic Image Quality," *Radiology*, vol. 190, no. 2, pp. 297–307, Feb. 1994.
- [2] Sylvia H Heywang-Köbrunner, D David Dershaw, and Ingrid Schreer, *Diagnostic Breast Imaging: Mammography, Sonography, Magnetic Resonance Imaging, and Interventional Procedures*, Georg Thieme Verlag, Stuttgart, Germany, 2nd, enlarged and revised edition, 2001.
- [3] Stephen H Taplin, Carolyn M Rutter, Charles Finder, Margaret T Mandelson, Florence Houn, and Emily White, "Screening mammography: Clinical image quality and the risk of interval breast cancer," *American Journal of Roentgenology*, vol. 178, pp. 797–803, Apr. 2002.
- [4] R Chandrasekhar, S M Kwok, and Y Attikiouzel, "Automatic evaluation of mammographic adequacy and quality on the mediolateral oblique view," in *Digital Mammography: IWDM 2002: 6th International Workshop on Digital Mammography*, Heinz-Otto Peitgen, Ed., pp. 182–186. Springer-Verlag, Heidelberg, Germany, 2003, Proceedings of the Workshop, June 22–25, 2002, Bremen, Germany.
- [5] R Chandrasekhar and Y Attikiouzel, "Automatic breast border segmentation by background modeling and subtraction," in *IWDM 2000: 5th International Workshop on Digital Mammography*, Martin J Yaffe, Ed., pp. 560–565. Medical Physics Publishing, Madison, WI, USA, 2001, Proceedings of the Workshop, June 11–14, 2000, Toronto, Canada.
- [6] Ramachandran Chandrasekhar and Yianni Attikiouzel, "A Simple Method for Automatically Locating the Nipple on Mammograms," *IEEE Transactions on Medical Imaging*, vol. 16, no. 5, pp. 483–494, Oct. 1997.
- [7] S M Kwok, R Chandrasekhar, and Y Attikiouzel, "Automatic pectoral muscle segmentation on mammograms by straight line estimation and cliff detection," in *Proceedings of the Seventh Australian and New Zealand Intelligent Information Systems Conference*, Perth, Western Australia, Nov. 2001, pp. 67–72, ARCME, The University of Western Australia.
- [8] J Suckling, J Parker, D R Dance, S Astley, I Hutt, C R M Boggis, I Ricketts, E Stamatakis, N Cerneaz, Siew-Li Kok, P Taylor, D Betal, and J Savage, "The Mammographic Image Analysis Society Digital Mammogram Database," in *Digital Mammography*, Alastair G Gale, Sue M Astley, David R Dance, and Alistair Y Cairns, Eds., Amsterdam, The Netherlands, 1994, vol. 1069 of *Excerpta Medica International Congress Series*, pp. 375–378, Elsevier Science.
- [9] S M Kwok, R Chandrasekhar, and Y Attikiouzel, "A mammogram-attribute database in XML format for data-driven segmentation and image analysis," in *IFMBE Proceedings: World Congress on Medical Physics and Biomedical Engineering (WC2003)*, Sydney, Australia, Aug. 2003, vol. 4, IFMBE and IOMP, 4 pages, CD-ROM, ISSN: 1727-1983.